

Control of the Nonthermal Electrons and Current Collapse at the Density Limit Disruption in T-10 Tokamak

P. V. Savrukhin 1), E.A.Shestakov1), D. V. Sarychev 1), A. V. Sushkov 1), S. A. Grashin 1), V. P. Budaev 1), S. G. Maltsev 1), Y. D. Pavlov 1)

1) Russian Research Center "Kurchatov Institute", 123182, Moscow, Russia

e-mail contact of main author: psavrukhin@bk.ru

ABSTRACT. Experiments in the T-10 tokamak ($R=1.5\text{m}$, $a=0.3\text{m}$) have demonstrated possibility of control of the non-thermal ($E>100\text{keV}$) electron generation and current decay rate after an energy quench at the density limit disruption using ECRH heating in combination with preprogrammed Ohmic power supply system and fast gas puffing. Application of the electron cyclotron waves allowed delaying and in some cases preventing formation of the nonthermal beams. Optimal conditions of safe termination of the plasma discharge using auxiliary heating are identified. System of external coils for generation of the resonant and stochastic magnetic fields is designed in the T-10 tokamak. Prospects of the system for control of the MHD modes and non-thermal electrons are analyzed using the phenomenological modeling.

1. Introduction

Safe termination of plasma discharge is one of the key problem in design of the plasma-facing components in tokamak reactor due to strong electromagnetic forces and enhanced heat fluxes arising during disruption instability and subsequent generation of the high energy (E up to 30MeV) “runaway” electron beams [1]. Several safe termination techniques were successfully demonstrated in tokamak experiments, including injection of massive gas jets, pellets, and dust (see [1,2]), and application of the external perturbed magnetic fields (see [3]). However, possibility of application of the techniques in a tokamak reactor needs further analysis. The problem is mainly connected with poor penetration of the neutral particles in high temperature plasma as well as with long time scale of the diffusion of the external magnetic fields through the blanket and first wall components.

Generation of the non-thermal electron beams in tokamak plasma is a complicated process affected by various kinetic and MHD phenomena. In simplified way production of the non-thermal beams can be represented by the diagram shown in Fig.1. The beams generation is driven by the primary runaway (Dreicer) acceleration and secondary knock-on avalanche, critically depending on the longitudinal electric field, E , and plasma parameters (e.g., electron temperature, T_e , and density, n_e) [1]. Dominant losses mechanism of the nonthermal electrons is generally determined by the macro-scale magnetic turbulence connected with MHD perturbations. Amplitude of the longitudinal electric field depends on the “equilibrium” plasma parameters ($E_0 \sim T_e^{-3/2}$) and on electric fields E^* induced during “transient” changes of the internal magnetic fluxes topology (e.g. magnetic reconnection, minor disruptions). Due to the transient nature of the induced electric fields their integral effect on the non-thermal electrons generation is generally neglected. However, analysis [4] indicated that during fast ($dt \sim 0.1\text{ms}$) disruption instability growth of the MHD modes and subsequent reconnection of the magnetic fluxes around the resonant magnetic surfaces can induce strong electric fields $E^* \gg E_0$ ($E^* = 10\text{-}50\text{V/m}$), which can facilitate production of the localized beams of the non-thermal electrons. Therefore, growth of the MHD modes could both induce losses and generation of the non-thermal electrons depending on growth rate and amplitude of the magnetic perturbations.

Control of the non-thermal electrons in tokamaks is generally provided by changing of the equilibrium plasma conditions (e.g. increasing of electron density by massive gas injection) or by application of the external magnetic perturbations (see, Ref. in [1-3]). Additional possibility was found in recent experiments in T-10 [5] demonstrated suppression of the non-thermal electrons by control of the MHD modes amplitude $\delta\Psi_{MHD}$ ($\delta\Psi_{MHD}$ - perturbed helical magnetic flux) and growth rate ($\delta\Psi_{MHD}/\delta t$) using ECRH (see, also [6,7]). It was demonstrated that suppression of the bursting MHD modes and setting of the saturated magnetic perturbations allowed complete elimination of the non-thermal electrons.

Present paper represents analysis of the T-10 experiments with suppression of the non-thermal electrons by control of the MHD modes using ECRH in various plasma conditions (Section.2). In order to additional study of the MHD modes effect on the non-thermal electrons, system of external coils producing resonant and stochastic magnetic fields is designed in the T-10 tokamak. General outline of the external coils system is described in Section.3. Prospects of the system for control of the MHD modes and non-thermal electrons and results of the experiments with ECRH are analysed using phenomenological model in Section.4.

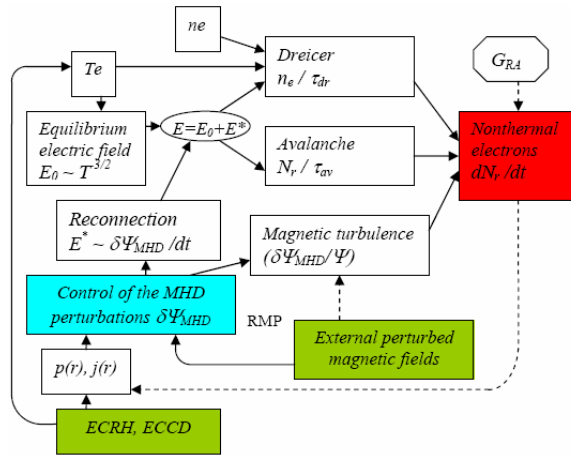


FIG. 1. Schematic view of the mechanisms leading to generation of the non-thermal electron beams in a tokamak plasma. Growth of the MHD modes and subsequent reconnection of the magnetic fluxes around the resonant magnetic surfaces can induce strong electric fields $E^* \gg E_0$, which can facilitate production of the localized beams of the non-thermal electrons, here E_0 is “equilibrium” longitudinal electric field. Control of the MHD modes using ECRH and Resonant Magnetic Perturbation can delay (suppress) production of the runaway beams. Plasma heating during ECRH can lead to decrease of the “equilibrium” electric field and subsequent reduction of the runaway beams.

2. Experimental results

Auxiliary heating (ECRH) system in T-10 consists of five gyrotrons with a total heating power of up to 2.5MW: 1.2MW at 130 GHz and 1.3MW at 140 GHz. An extraordinary wave on the 2nd ECR harmonic is launched from the low field side (LFS) in the direction of the major radius. The width of the ECRH power absorption profile is $\approx 2\%$ of the minor radius, power density up to 25 Wcm^{-3} is achievable. The cut-off densities are $n_{\text{cut-off}}(140 \text{ GHz}) \sim 1.2 \times 10^{20} \text{ m}^{-3}$ and $n_{\text{cut-off}}(130 \text{ GHz}) \sim 1 \times 10^{20} \text{ m}^{-3}$.

Non-thermal electrons are identified using tangential x-ray array (TX - array with CdTe detectors) placed inside the tokamak vacuum vessel at the low field side of the torus below the equatorial midplane and using in-vessel silicon AXUV-photodiode (Absolute eXtreme UltraViolet) detectors. The CdTe detectors provide measurements of the emissivity fluxes in energy range ($E_\gamma \sim 2.5\text{-}200 \text{ keV}$) with spatial and time resolution of order of $\delta r \sim 7 \text{ mm}$ and $3 \mu\text{s}$, accordingly. AXUV-photodiode detectors permit absolute radiated power measurements over range in photon energies $1\text{eV} < E < 6000 \text{ eV}$ with the nearly constant conversion efficiency (0.25 A/W) somewhat reduced in the region $1\text{eV} < E_{\text{ph}} < 30 \text{ eV}$. The diagnostic system consists of array of the 16 AXUV-photodiodes placed below the equatorial midplane. The field of view provides full plasma cross-section coverage ($-30 \text{ cm} \div 30 \text{ cm}$) with spatial resolution of order of 4 cm at the vessel midplane. Temporal resolution of the AXUV system

is 8 μ s. The hard x-ray radiation ($E_\gamma \sim 0.5-3$ MeV) is measured by the NaI(Tl) monitor placed outside the vacuum vessel.

Typical evolution of the plasma parameters in the experiment with density limit disruptions in T-10 ohmically heated plasma ($I_p=0.14$ MA, $B_t=2.4$ T) is shown in Fig. 2a. Additional gas puffing at $t=600$ ms leads to increase of the radiation power and growth of the MHD perturbations (dominant harmonic $m,n=2,1$). The process is terminated by the first energy quench ($t=670$ ms) with subsequent generation of an intensive “bursts” of the bolometric radiation and Da emission ($t=670-890$ ms). The process is accompanied by decay of the electron density and decrease of the plasma current ($t=670-970$ ms) and termination of the discharge by switch-off of the T-10 power supply system ($t>970$ ms). Analysis of the nonthermal x-ray radiation in similar plasma experiments [5] indicated that the “bursts” are connected with the non-thermal electrons generated periodically during magnetic reconnection in series of minor disruptions. Rate of the plasma current decay correlates with repetition rate of the bursts which indicates indirectly that current collapse in T-10 plasma is determined by the step-like process associated with the “reconnection events” inside the plasma core. Tomographic reconstruction of the non-thermal x-ray radiation using 2D CdTe detector arrays indicated that perturbation during initial stage of the density limit disruption are initiated in the plasma core and are later displaced to the plasma periphery.

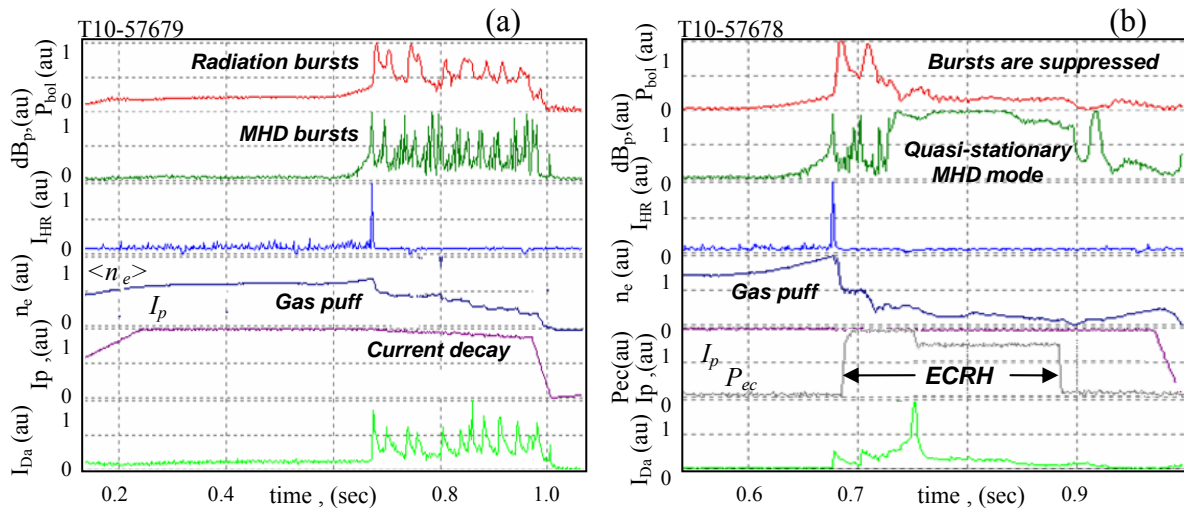


FIG. 2a. Time evolution of the plasma parameters during density limit disruption in Ohmically heated plasma. Here, P_{bol} – total radiated power, dB_p – poloidal magnetic field perturbations, I_{HR} – hard x-ray and neutron radiation, $\langle n_e \rangle$ – plasma density, I_p – plasma current, I_{Da} – intensity of the D_α radiation.

Fig.2b Time evolution of the plasma parameters during density limit disruption in plasma with ECRH heating ($P_{ec,abs}=1$ MW). The bursting MHD modes and the radiation bursts (see P_{bol}) connected with the nonthermal electrons are eliminated during whole duration of the ECRH pulse.

Auxiliary plasma heating using electron cyclotron waves leads to elimination of the bursting energy quenches and formation of the saturated MHD modes with “quasi-stationary” amplitude. This delay formation of the primarily nonthermal electrons, reduces the current decay rate, and in some cases assures restoration of the quasi-stable plasma conditions. Typical time evolution of the plasma parameters is shown in the case in Fig.2b and Fig.3. Radiation due to the nonthermal electrons is removed for the whole duration of the ECRH pulse and plasma current is sustained.

Effect of elimination of the bursting MHD modes and restoration of the hot plasma discharge is observed at relatively high ECRH power. The threshold power depends on position of the

ECRH zone across the plasma cross section (see Fig.4). The threshold power is decreased in discharges with low plasma current.

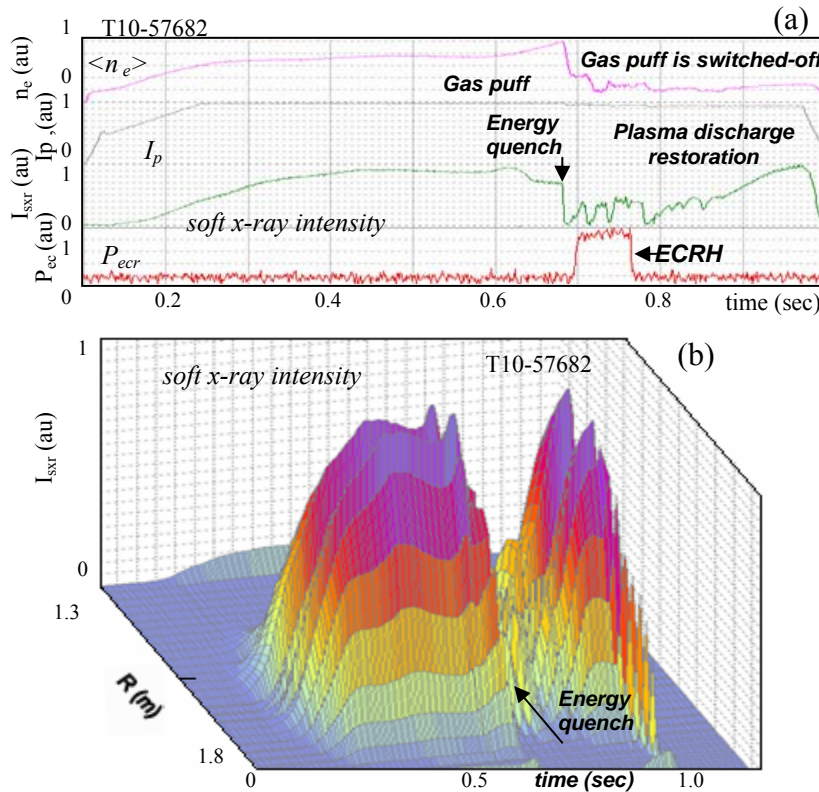


Fig.3a Time evolution of the plasma parameters in T-10 discharge with ECRH heating during the density limit disruption. Here, $\langle n_e \rangle$ - plasma density, I_p - plasma current, I_{sxr} - soft x-ray intensity, P_{ec} - ECRH power. Switching on of the auxiliary ECRH heating ($P_{ec,abs}=0.3MW$) after an energy quench facilitate restoration of the quasi-stable plasma operation.

Fig.3b Contour plot of the soft x-ray intensity measured by the multi-wire gas detector illustrating restoration of the hot plasma discharge ($t>0.8sec$) after an energy quench at $t=0.69sec$.

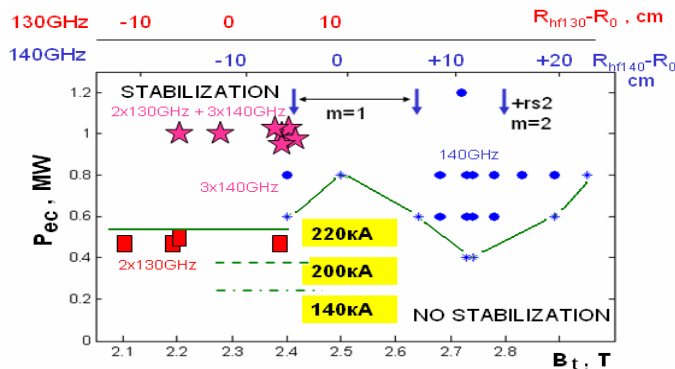


Fig.4. Diagram of the ECRH power required for elimination of the radiation bursts and suppression of the MHD modes in the T-10 plasma with various toroidal magnetic field (position of the EC resonance) and plasma currents. "Threshold" powers for plasma currents $I_p=230kA$, $I_p=200kA$, and $I_p=140kA$ are shown schematically by solid, dashed, and dotted-dashed lines.

3. System of external windings for resonant magnetic field perturbations and plasma stochastization

System of external coils is designed in the T-10 tokamak (Fig.5). The system consists of eight saddle coils placed above and below the equatorial midplane and set of sixteen circular coils placed along the toroidal circumference of the torus symmetrically around the equatorial midplane. The saddle coils produces quadruple magnetic field resonant with the low- m,n MHD perturbations (see Fig.6), while circular coils are used for stochastization of the plasma periphery at the low field side of the torus.

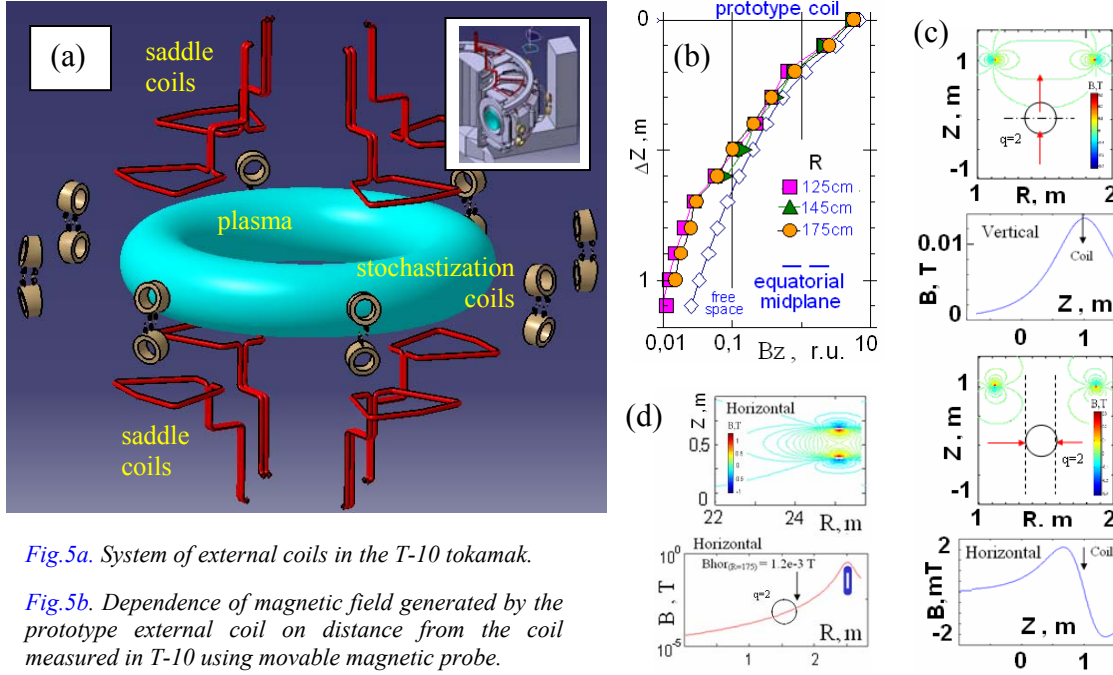


Fig.5a. System of external coils in the T-10 tokamak.

Fig.5b. Dependence of magnetic field generated by the prototype external coil on distance from the coil measured in T-10 using movable magnetic probe.

Fig.5c,d Calculated perturbed magnetic field produced by singular saddle coil (c) and circular coil (d) around the $q=2$ surface (marked by circle).

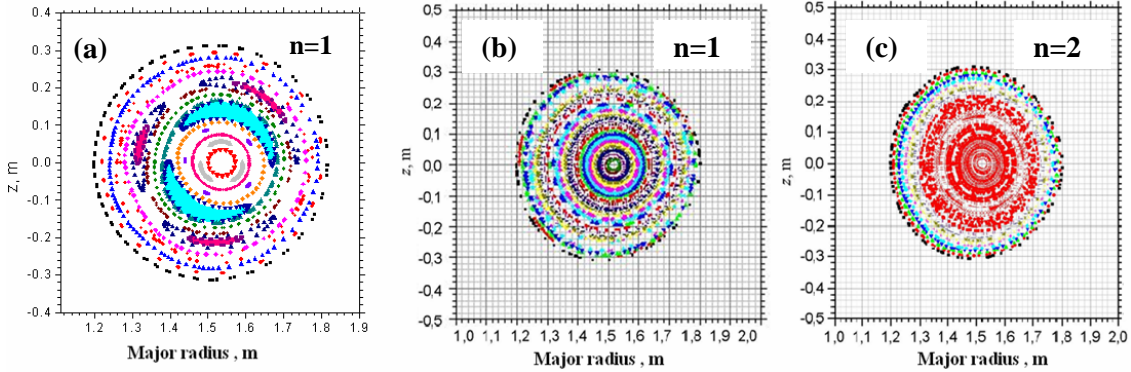


Fig.6. Plot of the magnetic field in the T-10 tokamak in various plasma conditions calculated during application of the external field produced by saddle coils: (a) $I_p=0.075\text{MA}$, $\beta_p=0.6$, $l_i=1.5$, $B_i=1.5\text{T}$. (b,c) $I_p=0.3\text{MA}$, $\beta_p=0.5$, $l_i=1.0$, $B_i=2.4\text{T}$. Polarity of currents in the saddle coils ($I_{sc}=0.05\text{MA}\cdot\text{turns}$) is selected to produce $n=1$ (a,b) and $n=2$ (c) dominant harmonics.

4. Phenomenological model of the non-thermal electrons control

Time evolution of the density of the nonthermal electrons (N_r) generated by the electric field (E) in a thermal plasma with density n_e can be described by the equation (see Ref. in [1,4]): $\partial N_r / \partial t + \nabla \cdot (\mathbf{v}_r N_r) = n_e / \tau_{dr} + N_r / \tau_{av} - \nabla \Gamma_{loss}$, where, $|\mathbf{v}_r| \sim 0.5c$ is the nonthermal electron mean velocity, $1/\tau_{dr}$ and $1/\tau_{av}$ are the production rates of the primary runaway electrons (Dreicer acceleration) and secondary knock-on avalanche, accordingly, and flux Γ_{loss} denotes losses of the nonthermal electrons. Here, $\tau_{dr}^{-1} \approx 0.3 v_e \varepsilon_d^{-3(Z_{eff}+1)/16} \exp(-1/4\varepsilon_d - ([Z_{eff}+1]/\varepsilon_d)^{1/2})$, where $\varepsilon_d = E/E_c$, E_c is the critical (threshold) electric field given by $E_c = e^3 n_e Z_{eff} \ln \Lambda / (4\pi \varepsilon_0^2 m_e v_{th}^2)$, v_e is the collision frequency of the electrons at the thermal velocity v_{th} , Z_{eff} is the effective plasma charge ($Z_{eff} \approx 1$) and $\tau_{av}^{-1} \approx 2m_e c \ln \Lambda a(Z_{eff}) / (eE)$, where $a(Z_{eff}=1) \approx 1$. It was established

in previous studies that macroscale magnetic turbulence constitutes the dominant losses mechanism of the nonthermal electrons during the process. Such losses can be represented by the flux $|I_{loss}| = D_{rt} \partial N_r / \partial r$, where the diffusion coefficient D_{rt} is determined by the normalised amplitude of magnetic field perturbations B_r/B_t : $D_{rt} \approx (\pi R_0 q v_r) (B_r/B_t)^2$. The magnetic field perturbations are represented by a radial function decaying outside the resonant magnetic surface: $B_r = (r_s/r)^{m+1} B_r$. Growth of the MHD mode during the disruption leads to squeezing the magnetic field lines with different pitch angles around the resonant surface with subsequent reconnection of the perturbed magnetic fluxes. Amplitude of the electric field induced in the process can be determined by the rate of change of the perturbed magnetic fields inside the current layer with width δ_{rec} around the resonant surface: $E^* \sim \delta_{rec} dB_r/dt$.

Magnetic field perturbations in the simulations are represented by small non-linear disturbances of the radial magnetic field superimposed to the equilibrium configuration: $b_{rm} = B_r \exp(jm\chi_{im})$, where $\chi_{im} = m\theta - n\phi + \int \omega_{im}(t') dt'$, ω_{im} are phase and instantaneous frequency of the mode, and ϕ is the longitudinal coordinate. Dynamic of only single $m=2, n=1$ harmonic is considered in the present paper. This approach is justified as soon as this harmonic is dominant in the experiments in T-10. Detailed analysis of the coupled tearing modes is made elsewhere (see references in [8,9]).

Following the theory (see Ref. in [1,8]), dynamic of the magnetic perturbations at the resonance surface $r=r_{s2}$ are entered two distinctive regimes subject to the bulk plasma parameters (viscosity, inertia, and resistivity) and amplitude of the magnetic perturbations. Transition between two regimes depends on the parameter $\lambda = (\delta_l/w_i)^{3/2}$, where $\delta_l = \tau_H^{2/6} (\tau_V \tau_R)^{-1/6} r_{s2}$ is the linear layer width for visco-resistive tearing mode driven by the external magnetic field, $w_i = 4r_{s2} (B_r/2 / (s_{s2} B_{\theta 0} m))^{1/2}$ - width of the ‘magnetic island’. Here, $\tau_R = \mu_0 r_{s2}^2 / \eta_2$, $\tau_V = \rho_2 r_{s2}^2 / \mu_{v2}$, $\tau_H = R_0 (\mu_0 \rho_2)^{1/2} / (s_{s2} B_{z0})$ are resistive, viscous, and hydromagnetic time scales accordingly, η_2 - coefficient of the parallel resistivity; B_{z0} and $B_{\theta 0}$ are longitudinal and poloidal component of the equilibrium magnetic field, s_{s2} - magnetic shear ($s_s = (r/q) dq/dr$) at the $q=2$ surface, μ_{v2} is anomalous coefficient of perpendicular viscosity (see bellow), and $\rho_2 = n_{e2} A m_p$ is mass density. Magnetic island is assumed suppressed till amplitude of the magnetic perturbations overcome threshold amplitude: $B_l = c_l s_{s2} \delta_l^2 B_{\theta 0} / (8r_s^2)$. Here, c_l is numerical parameter chosen in the simulations to fit the experimental data (see [9]).

Dynamic of the MHD perturbations in the non-linear regime ($\lambda < 1$) is described by theory of the non-linear tearing modes (see [1,8]). Stability of the tearing mode is determined by analysis of the marginally stable ideal MHD equilibrium subject of the current density profile with the boundary conditions specified by the controlled currents in saddle coils and image currents in the vessel.

In polar co-ordinates rotated with the magnetic island growth of the magnetic perturbations is described by equation: $dB_{r2}/dt = c_{mg3} ([\Delta'_{fbr} - c_{mg5} (\omega_{i2} \tau_{ves})^2 (f_2 + (\omega_{i2} \tau_{ves}))^2 f_2^{-1/2}] B_{r2}^{1/2} + c_{mg4} (B_{ed2} + B_{errd2}) B_{r2}^{-1/2})$. Here, Δ'_{fbr} is stability parameter of the free-boundary tearing mode, $c_{mg3} = 1.2 \eta_2 (B_{\theta 0} s_{s2})^{1/2} / (\mu_0 r_{s2})$, $c_{mg4} = 4/r_{s2}$, $c_{mg5} = 4/r_{s2} (r_{s2}/r_v)^4$, $f_2 = (1 - (r_{s2}/r_v)^4)^{-2}$, τ_{ves} is time constant of the vessel represented in the model as hollow cylinder with inner radius $r=r_v$, and B_{ed2}, B_{errd2} are amplitudes of the ‘direct’ (see bellow) components of the $m=2$ harmonics of the controlled and the intrinsic error fields accordingly. All the parameters are evaluated at the $q=2$ magnetic surface ($r=r_{s2}$). Function ω_{i2} represents instantaneous angular frequency of the magnetic island.

According with the theory, term Δ'_{fbr} is a complicated function of the plasma parameters. In a simplified way it is specified by relation (see [1,8]): $\Delta'_{fbr} = c_{mg2} (1 - c_{mg1} B_{r2}^{1/2}) + \Delta'_{heat}$, where, c_{mg1} is numerical coefficient specifying ‘phenomenological’ amplitude of the non-linearly

saturated magnetic island and $c_{mg2} \equiv \Delta'_0$ is the tearing mode stability parameter in the equilibrium plasma. Term Δ'_{heat} represents effect of the auxiliary heating on plasma conductivity within the magnetic island. The effect depends on localization of the absorbed auxiliary power profile in respect to the magnetic island localization. Assuming Gaussian profile of the auxiliary power profile: $\delta P_{aux} = P_{aux} \exp(-(r - r_{aux})^2 / \delta r_{aux}^2) \exp(-(\chi_{im} - \chi_{aux})^2 / \delta \chi_{aux}^2)$, and considering power absorption within the magnetic island ($\delta r_{aux} < W_i$) one can obtain (see Ref. in [1]): $\Delta'_{heat} = -24 w_i / (s k_{\perp} T_e) dP_{aux}$. Here, dP_{aux} – total power of the auxiliary heating absorbed in area with r_{aux} , χ_{aux} , δr_{aux} , $\delta \chi_{aux}$ radial and angular localization coordinates and k_{\perp} - coefficient of the transverse electron heat diffusivity.

Angular motion (rotation) of the MHD modes is determined in the simulations by balance of the driving torque due to viscous coupling between fluid confined with the magnetic perturbations and the surrounding plasma fluid and the electromagnetic torques due to interaction of the mode with the image currents in the vessel and due to effects from the externally applied controlled and error magnetic fields: $c_{r2} d\omega_{i2} / dt = c_{r4} (\omega_{p2} - \omega_{i2}) - c_{r1} B_{r2}^2 f_2 \omega_{i2} \tau_{ves} / (f_2 + (\omega_{i2} \tau_{ves})^2) + c_{r3} B_{r2} (B_{eq2} + B_{errq2})$, $d\chi_{i2} / dt = \omega_{i2}$. Here, $c_{r1} \equiv 2\pi^2 r_{s2}^6 R_0 / (\mu_0 r_v^2)$, c_{r2} - ‘phenomenological’ moment of inertia of the plasma confined inside magnetic perturbations, $cr3 \equiv 4\pi^2 r_{s2}^2 R_0 / \mu_0$, $cr4 \equiv 4\pi^2 r_{s2} R_0^3 \rho_2 \mu_{v2} / d_{v2}$ - coefficient of the viscous friction, d_{v2} - width of the viscous layer, and B_{eq2} , B_{errq2} , are amplitudes of the quadrature components of the $m=2$ harmonics of the controlled and intrinsic error magnetic fields accordingly, ω_{p2} is frequency of the plasma fluid surrounding magnetic island. Only rotation in the toroidal direction is considered in the model (see [8,9]).

Toroidal rotation of the ‘phenomenological’ fluid (bulk plasma) surrounding magnetic island is assumed proportional to the angular rotation of the ion fluid.

External magnetic field in the reference frame rotated with the specified tearing mode is determined by direct B_{eD} and quadrature B_{eQ} components of the external field in the static reference frame: $B_e = B_{eD} \cos(m\theta - n\phi) + B_{eQ} \sin(m\theta - n\phi)$. Components of the external field in the static reference frame are calculated by integration and Fourier decomposition of the magnetic field at specified resonance surface generated by currents in saddle coils after correction for the screening effect from the vessel.

Stability of the tearing mode (Δ'_{frib}) is analysed by MHD equilibrium code subject to the current density profile. Effect of the MHD modes on electron temperature profile is simulated using simplified energy balance equation with periodic enhancement of the electron heat diffusivity proportional to amplitude of the mode. Results of numerical simulations of the tearing mode and effect of the ECRH and externally applied magnetic field are shown in Fig.7.

5. Conclusions

In conclusion, bursts of the nonthermal x-ray intensity and radiation is observed in T-10 plasma during current decay stage of the density limit disruptions. Analysis indicated that the bursts can be connected with nonthermal electrons generated during magnetic reconnection in series of minor disruptions. Accordingly with results of numerical modelling such periodic generation of the nonthermal electrons can facilitate production of the runaway beams. Application of the ECRH heating allows delaying and in some cases preventing generation of the primarily nonthermal electrons and restoration of the ‘quasi-stable’ plasma discharge. Numerical modelling indicated that this effect can be connected with modification of the equilibrium current density and pressure profiles with subsequent control of MHD modes growth rate and amplitude.

Acknowledgements

The work is supported by Russian Atomic Energy Agency ROSATOM and RFBR 08-02-01345.

References:

- [1] ITER Physics Expert Group on Disruptions, Plasma Control, and MHD, ITER Physics Basis Editors, Nucl. Fusion 39, (1999) 2251.
- [2] M.N. Rosenbluth, S.V. Putvinskij, P.B. Parks, Liquid jets for fast plasma termination in tokamaks, Nucl. Fusion 37 (1997) 955.
- [3] R.Yoshino, et al., Nucl. Fusion 40, 1293 (2000).
- [4] P.V.Savrukhin. Physics of Plasmas, 9 (2002) 3421.
- [5] P.V.Savrukhin and the T-10 Group, In.Proc. 22nd IAEA Fusion Energy Conference FEC 2008, Geneva, IAEA/EX/7-3Rc (2008).
- [6] P.V.Savrukhin, et al., Nucl. Fusion 34 (1994) 317.
- [7] B.Esposito, Nucl. Fusion (2009) 304326.
- [8] D.Biskamp, Nonlinear magnetohydrodynamic, Cambridge University Press, Cambridge (1993).
- [9] Savrukhin P., et al., JET Report, Abingdon, JET-R(95)-06., 1995.

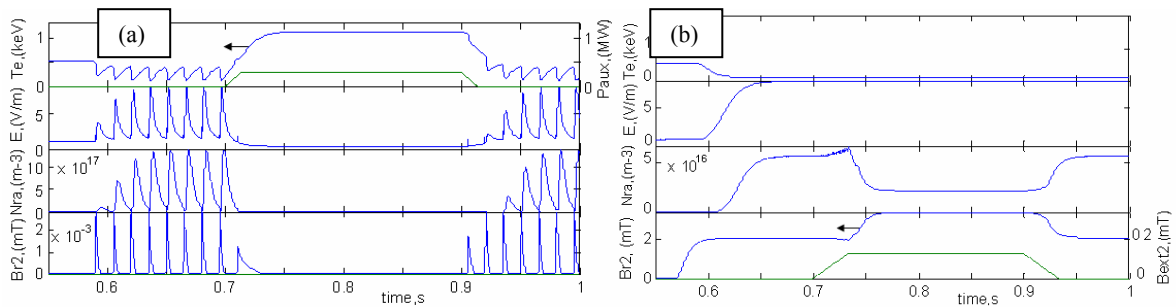


FIG. 7. Numerical modeling of the nonthermal electron beams in the T-10 plasma with application of the ECRH (a) and externally applied resonant magnetic field (b). Here, shown: electron temperature, T_e , longitudinal electric field, E , density of the nonthermal beam, N_{ra} , amplitude of the magnetic perturbations, Br_2 , power of ECRH heating, P_{aux} , and amplitude of the controlled magnetic field B_{ext2} .